

Metal–insulator transition in Ni-doped $\text{Na}_{0.75}\text{CoO}_2$: Insights from infrared studies

M PREMILA, A BHARATHI, N GAYATHRI, P YASODHA, Y HARIHARAN and
C S SUNDAR*

Materials Science Division, Indira Gandhi Centre for Atomic Research,
Kalpakkam 603 102, India

*E-mail: css@igcar.gov.in

Abstract. Nickel substitution at the cobalt site in $\text{Na}_{0.75}\text{CoO}_2$ induces an upturn in the resistivity on lowering the temperature, with the metal-to-insulator transition temperature (T_{MIT}) increasing with the Ni content. Low temperature far infrared measurements on polycrystalline samples of $\text{Na}_{0.75}\text{CoO}_2$ and $\text{Na}_{0.75}\text{Co}_{0.95}\text{Ni}_{0.05}\text{O}_2$, the latter having $T_{\text{MIT}} \sim 175$ K, have been carried out. Dramatic changes in the Na mode frequencies, and relative intensities of the out-of-plane modes corresponding to the two Na sites are observed, coincident with the MIT in $\text{Na}_{0.75}\text{Co}_{0.95}\text{Ni}_{0.05}\text{O}_2$. It is argued that these changes are associated with a charge ordering of the CoO_2 layer, associated with the metal–insulator transition.

Keywords. Sodium cobaltate; metal–insulator transition; charge ordering; sodium modes; infrared spectroscopy.

PACS Nos 71.27.+a; 74.25.Fy; 78.30.-j; 71.30.+h

1. Introduction

The sodium cobaltate system, Na_xCoO_2 , in which the Co ions define a layered triangular lattice, with Na ions sandwiched between the CoO_2 layers, has evoked considerable interest due to the large thermopower for $x \sim 0.7$ [1] and superconductivity in water intercalated system with $x \sim 0.3$ [2]. The phase diagram of Na_xCoO_2 is rich, replete with a variety of ground states [3]. For $1/4 < x < 1/3$ the system is a paramagnetic metal, that becomes superconducting with water intercalation [2]. For $x = 0.5$, the system is a charge ordered insulator. One of the interesting aspects of the phase diagram is for $x \sim 0.7$, the system is metallic while exhibiting a Curie–Weiss behaviour [3]. This is also the composition regime where the system has a large thermopower, that is attributed to spin transport [1]. In this composition regime, at low temperatures, magnetic transitions have been observed. In addition to studies with varying Na stoichiometry, which in turn determines the $\text{Co}^{3+}/\text{Co}^{4+}$ ratio, there have been several studies on doping the CoO_2 layer. It has been seen that substitutions of transition metals like Ni [4], Mn [5] and Ir [6] in place of Co, induces a metal-to-insulator transition even while the Na content

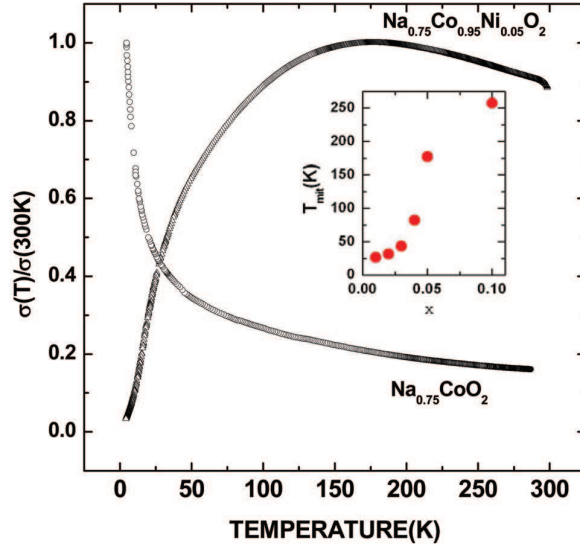


Figure 1. Variation of conductivity $\sigma(T)$, normalized to the respective 300 K values, as a function of temperature in $\text{Na}_{0.75}\text{CoO}_2$ and $\text{Na}_{0.75}\text{Co}_{0.95}\text{Ni}_{0.05}\text{O}_2$. The Ni-doped sample is seen to change over from a metallic to insulating behaviour at ~ 175 K. The inset shows the increase of the metal-insulator transition, T_{MIT} , with Ni content, x , in $\text{Na}_{0.75}\text{Co}_{1-x}\text{Ni}_x\text{O}_2$ (from ref. [4]).

$x \sim 0.75$. In all the substituted systems studied, the smallest concentration of impurity atom suffices to induce a metal-insulator transition (MIT).

Our investigations [4] are on the influence of Ni doping of the CoO_2 layer, that has been probed by resistivity and thermopower measurements as a function of temperature. Addition of Ni is seen to promote the formation of an insulating ground state with the metal-to-insulator transition temperature, T_{MIT} , increasing with the Ni content (see figure 1). In order to see if the MIT is associated with a magnetic transition, magnetization measurements at low temperatures have been carried out, but no magnetic anomaly was observed [4]. It is of interest to see if the transition to the insulating phase is associated with a charge ordering transition, since charge ordering in the CoO_2 layer is another major instability in these materials [7,8]. Charge ordering has been addressed using various techniques like neutron diffraction [9,10], electron diffraction [3,11], NMR [12], PES [13] and optical studies including both Raman [14,15] and infrared spectroscopy [7,16–20].

In the present work we report the low temperature (300–77 K) far-infrared absorption measurements on polycrystalline samples of $\text{Na}_{0.75}\text{CoO}_2$ and $\text{Na}_{0.75}\text{Co}_{0.95}\text{Ni}_{0.05}\text{O}_2$ ($T_{\text{MIT}} \sim 175$ K) pelletized in CsI matrix. Here we follow both the low-frequency sodium modes and the high-frequency Co vibration modes across the T_{MIT} . We observe significant changes in the Na mode frequencies and the relative intensities of modes corresponding to the Na sites, that is correlated with the MIT in the Ni-doped sample. We argue that this change in the preferential site occupancy of the sodium ions is indicative of the charge ordering of the CoO_2 layer in Ni-doped $\text{Na}_{0.75}\text{CoO}_2$.

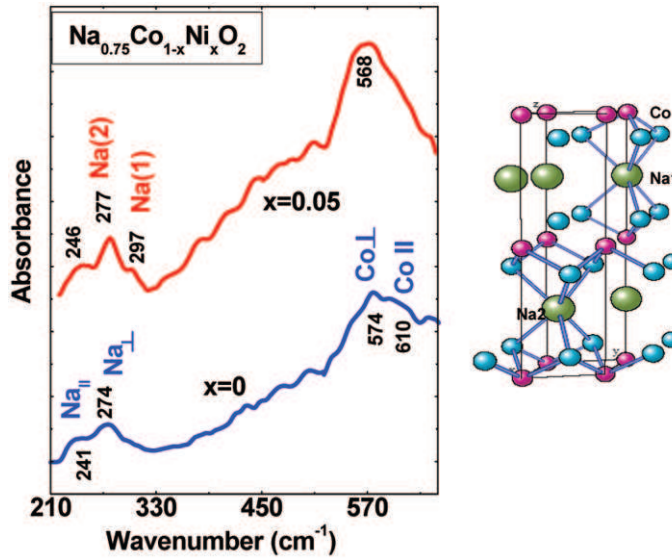


Figure 2. Infrared spectra at room temperature in $\text{Na}_{0.75}\text{CoO}_2$ and $\text{Na}_{0.75}\text{Co}_{0.95}\text{Ni}_{0.05}\text{O}_2$. The Na and Co modes, parallel and perpendicular to the c -axis are indicated. The right panel shows the crystal structure with the identification of the two Na sites, Na(1) and Na(2).

2. Experimental details

Polycrystalline samples of $\text{Na}_{0.75}\text{CoO}_2$ and $\text{Na}_{0.75}\text{Co}_{0.95}\text{Ni}_{0.05}\text{O}_2$ have been prepared by mixing stoichiometric proportions of Na_2CO_3 , Co_3O_4 and NiO and subjecting them to an initial calcination at 600°C for 12 h followed by subsequent pelletization and sintering at 800°C for 20 h. A final heat treatment at 850°C for 20 h was carried out to improve grain connectivity. Resistivity measurements using the four probe technique were carried out in a dipstick cryostat in the temperature range 300–4.2 K [4]. Far-infrared FTIR absorption measurements were carried out on well-characterized powder samples using a Bomem DA8 spectrophotometer operating with a resolution of 4 cm^{-1} in the range 30–900 cm^{-1} . Measurements were done using an extended 6 micron mylar beamsplitter in combination with a deuterated triglycine sulfate detector on samples pelletized with CsI. For experiments involving temperature variation of the infrared modes, the pellets were mounted inside a JANIS continuous flow cryostat and studies in the temperature range 300–77 K were carried out.

3. Infrared spectra and mode assignments

Figure 2 shows the infrared absorption spectra in $\text{Na}_{0.75}\text{CoO}_2$ and $\text{Na}_{0.75}\text{Co}_{0.95}\text{Ni}_{0.05}\text{O}_2$. The crystal structure (space group: $P6_3/mmc$) with the two Na sites indicated, is shown in the right panel. Factor group analysis predicts four infrared

active optical phonons for the system Na_xCoO_2 : $\Gamma_{\text{IR}} = 2E_{1u} + 2A_{2u}$ [21]. In $\text{Na}_{0.75}\text{CoO}_2$, absorption features are seen at 241, 274, 574 and 610 cm^{-1} . In the assignment of the modes, we take support from the first principles lattice dynamical calculations [21] that have been carried out for NaCoO_2 , with complete occupancy of Na at Na(1) and Na(2) sites. According to these calculations, the IR active modes, corresponding to various Na and Co vibrations for Na occupancy at Na(1) and Na(2) sites (whose numbers indicated in parenthesis) are as follows: $\text{Na}_{\text{in-plane}} (E_{1u})$: 201 (216) cm^{-1} , $\text{Na}_{\text{out-of-plane}} (A_{2u})$: 397 (337) cm^{-1} , $\text{Co}_{\text{in-plane}} (E_{1u})$: 587 (590) cm^{-1} and $\text{Co}_{\text{out-of-plane}} (A_{2u})$: 569 (566) cm^{-1} . While the theoretical calculations [21] do not provide one-to-one correspondence with the observed infrared features seen in figure 2, it helps to assign the modes as follows: The absorption features at 241 and 274 cm^{-1} are associated with the in-plane and out-of-plane vibrations of Na. Correspondingly, the high-frequency absorption features at 574 and 610 cm^{-1} are associated with the out-of-plane and in-plane vibrations of cobalt. It may be remarked that the two low-frequency sodium modes have been discerned for the first time in this infrared absorption experiments, while in the earlier infrared reflectivity measurements [7,16–20] only the high frequency optical phonon at ~ 570 cm^{-1} , corresponding to Co–O vibrations, was evident.

In the Ni-doped samples, the out-of-plane vibrations of Na, is seen to develop a shoulder at 297 cm^{-1} . We assign the harder mode at 297 cm^{-1} to Na at Na(1) site and the softer mode at 277 cm^{-1} to Na(2) site. This could be rationalized based on the structure, as also theoretical calculations [21]. Neutron scattering measurements [9] on $\text{Na}_{0.7}\text{CoO}_2$ samples indicate occupancy of Na(2) and Na(1) sites in the ratio of 0.5:0.2, and the observed intensity ratios of the modes at 277 and 297 cm^{-1} is consistent with this, lending credence to the above assignment. In contrast to the out-of-plane vibrations, the in-plane sodium vibrations at a lower frequency (~ 241 cm^{-1}) does not show any discernible splitting. This could be expected as the in-plane vibrations of Na is not very different for Na(1) and Na(2) sites [21]. However, in the studies on temperature dependence of Na modes (see below) we analyse the Na modes in terms of four components: the in-plane and out-of-plane vibrations, corresponding to the occupancy of Na at Na(1) and Na(2) sites.

4. Temperature dependence of sodium modes

The temperature dependence of infrared absorption spectra is shown in figure 3. The right panel shows the evolution of Na modes in detail. Figure 4 shows the decomposition of Na modes into four components: ν_1, ν_2, ν_3 and ν_4 , the former two corresponding to in-plane vibrations and the latter two due to out-of-plane vibrations. The higher and lower frequencies of each pair correspond to Na(1) and Na(2) site occupancies. The right panel shows the temperature dependence of these mode frequencies in $\text{Na}_{0.75}\text{CoO}_2$ and $\text{Na}_{0.75}\text{Co}_{0.95}\text{Ni}_{0.05}\text{O}_2$. Clearly, in the case of Ni-doped sample, the out-of-plane vibrations exhibit anomalous changes in the mode frequency that correlates well with T_{MIT} . Subtle changes are also seen in the in-plane modes. In contrast, the corresponding sodium modes of the undoped sample shows a regular anharmonic temperature dependence. It is also seen from

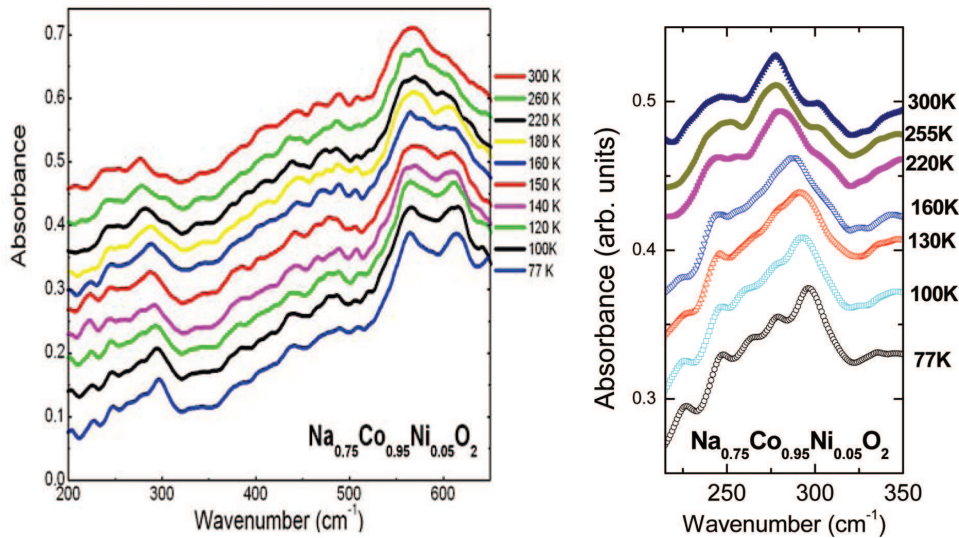


Figure 3. Temperature dependence of infrared absorption in $\text{Na}_{0.75}\text{Co}_{0.95}\text{Ni}_{0.05}\text{O}_2$. The Co modes, centred at $\sim 570\text{ cm}^{-1}$ are seen to split with the lowering of temperature. The evolution of the Na modes is shown in the right panel.

figure 4, that apart from changes in the mode frequencies with temperature, there are also interesting changes in the intensities of the modes. For example, there is a build up in the intensity of the ν_4 mode at the expense of ν_3 mode as the temperature is lowered. This is shown in detail in figure 5, where the evolution of the spectra in the region of ν_3 and ν_4 modes, that correspond to the out-of-plane vibrations of Na modes, is shown. With the lowering of temperature, the intensity of the mode at 297 cm^{-1} , that corresponds to the out-of-plane vibrations at Na(1) site, builds at the cost of the intensity of the mode at 277 cm^{-1} , corresponding to Na(2) site. The temperature dependence of the area under the two peaks (fitted to Gaussians) is shown in the right panel, and this indicates a dramatic flipping of intensities, that correlates excellently with $T_{\text{MIT}} \sim 175\text{ K}$. These observations clearly indicate that in $\text{Na}_{0.75}\text{Co}_{0.95}\text{Ni}_{0.05}\text{O}_2$, below the metal-to-insulator transition, the Na(1) becomes the preferred site for sodium ions, whereas in the metallic state the preferred site is Na(2) (see also figure 2). This, at the outset is surprising, since the sodium ions at Na(1) site is directly below the Co ion.

5. Behaviour of cobalt modes

It is seen from figure 3 that with the lowering of temperature, the broad feature at 570 cm^{-1} , that corresponds to CoO_6 vibrations, gets split into two distinctive peaks. Such a behaviour of the Co–O mode has earlier been seen [18] in $\text{Na}_{0.82}\text{CoO}_2$ and has been attributed to charge ordering within the CoO_2 layers. In order to see

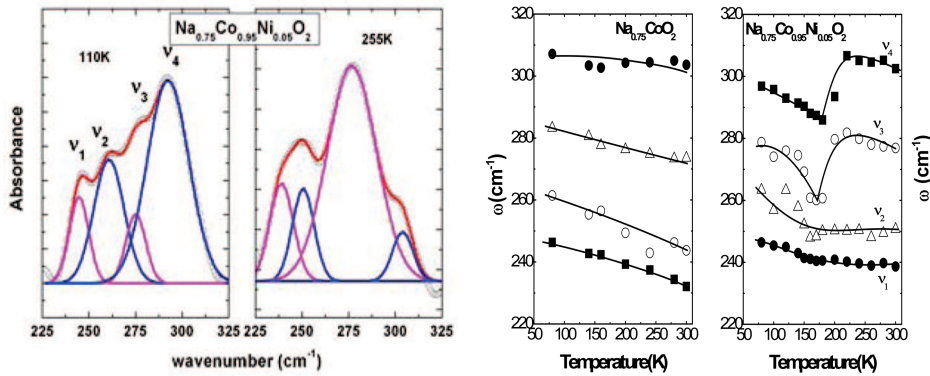


Figure 4. Four-component fits to the infrared absorption spectra in $\text{Na}_{0.75}\text{Co}_{0.95}\text{Ni}_{0.05}\text{O}_2$, in the region corresponding to Na vibrations, are shown in the left panel. The right panel shows the results of such analysis. The temperature dependence of Na mode frequencies in $\text{Na}_{0.75}\text{Co}_{0.95}\text{Ni}_{0.05}\text{O}_2$ shows distinctive changes associated with the metal-insulator transition, whereas regular anharmonic behaviour is seen in $\text{Na}_{0.75}\text{CoO}_2$.

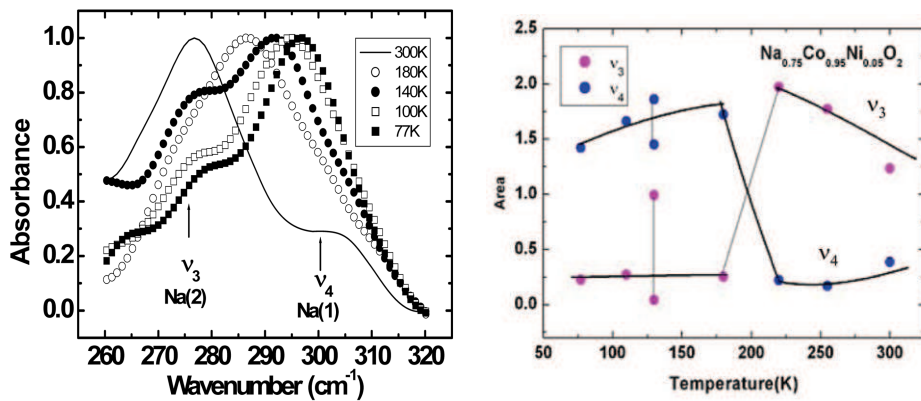


Figure 5. Temperature dependence of infrared absorption spectra in $\text{Na}_{0.75}\text{Co}_{0.95}\text{Ni}_{0.05}\text{O}_2$ in the region corresponding to out-of-plane vibrations of Na atoms at Na(1) and Na(2) sites (see figure 2). A build up of the intensity of the ν_4 mode, that corresponds to Na at Na(1) site, at the expense of the ν_3 mode, that corresponds to Na at Na(2) site, is seen. The right panel shows the dramatic flipping of the areas corresponding to the ν_3 and ν_4 modes, that coincides with the metal-to-insulator transition.

if the splitting of modes, seen in figure 3, is related to the metal-insulator transition or is just a consequence of the narrowing of modes with lowering of temperature, we have analysed this feature in terms of two components. These two components correspond to in-plane and out-of-plane vibrations of CoO_6 . Figure 6 shows a comparison of the variation of cobalt modes in $\text{Na}_{0.75}\text{Co}_{0.95}\text{Ni}_{0.05}\text{O}_2$, that undergoes a metal-to-insulator transition at 175 K and $\text{Na}_{0.75}\text{CoO}_2$ that remains metallic at low

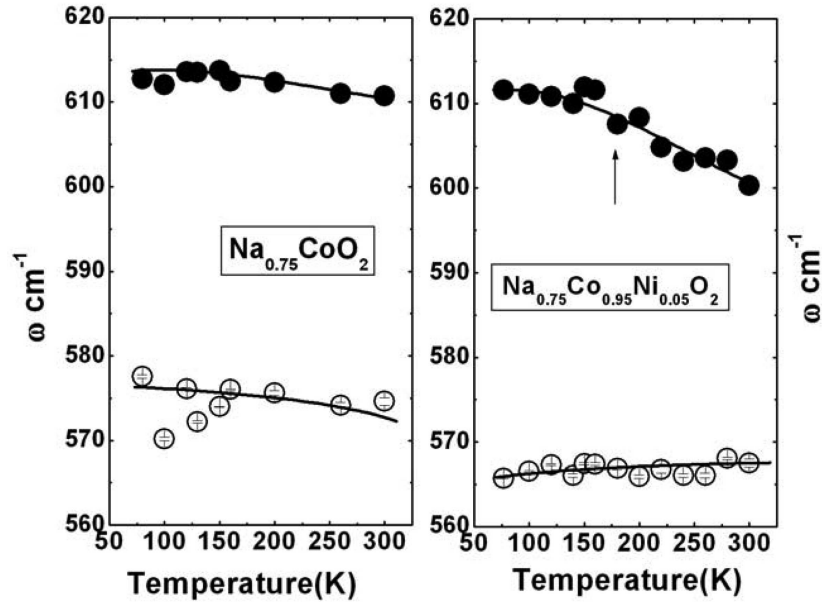


Figure 6. Temperature dependence of cobalt modes in $\text{Na}_{0.75}\text{CoO}_2$ and $\text{Na}_{0.75}\text{Co}_{0.95}\text{Ni}_{0.05}\text{O}_2$. The arrow indicates the metal-insulator transition temperature.

temperatures. No distinctive changes (unlike the Na modes, discussed earlier), that can be associated with the metal-to-insulator transition, is seen. The temperature dependence of mode frequencies in both the undoped and Ni-doped systems are reminiscent of regular anharmonic behaviour. We have also examined the trends in widths of these modes (figure not shown), and these too do not show any features that could be correlated with the MIT.

6. Discussions

It is seen from results presented so far that the out-of-plane Na mode frequencies and their relative intensities show distinctive changes that could be correlated with the MIT in $\text{Na}_{0.75}\text{Co}_{0.95}\text{Ni}_{0.05}\text{O}_2$. These changes in infrared mode frequencies imply changes in structural features, associated with the MIT. As indicated earlier, charge ordering is a possible instability in this sodium cobaltate system, and we would like to explore if the observed changes in infrared spectra is indicative of this.

Charge ordering has been seen for the composition $\text{Na}_{0.5}\text{CoO}_2$, in which it has been shown unambiguously that the insulating state is associated with charge ordering of the Co sub-lattice into rows of Co^{3+} and Co^{4+} , which in turn gives rise to an ordering of the Na atom positions into zig-zag chains avoiding proximity of Na atoms to the Co^{4+} ions [7,9,11]. Figure 7a shows the schematic of the underlying triangular lattice of Co ions, with the distribution of Na atoms at Na(1) site, that is above the Co ion, and the Na(2) site that is at the centres of triangles. In the metallic state there is a random distribution of the Co^{3+} and Co^{4+} ions with the

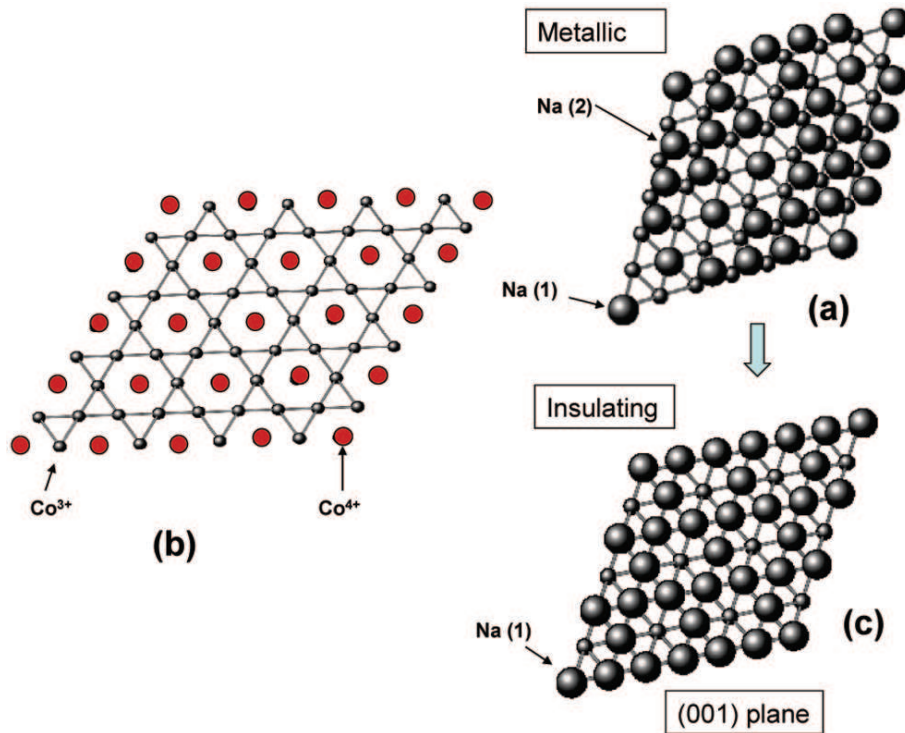


Figure 7. Schematic of the charge ordering of the Co layer and corresponding change in the Na occupancy. (a) Projection in the (0 0 1) plane, showing a random arrangement of Co^{3+} and Co^{4+} ions (both indicated as small spheres) on a triangular lattice in the metallic phase. The position of Na atoms (large spheres) corresponding to Na(1) and Na(2) sites is shown. (b) The charge ordering of Co^{3+} ions (connected full circle) and Co^{4+} ions (unconnected open circle) in a Kagome lattice for $\text{Na}_{0.75}\text{CoO}_2$. To avoid proximity to Co^{4+} ions, Na moves from Na(2) to Na(1) position, in the charge ordered insulating phase, as shown in panel (c).

$\text{Co}^{3+}/\text{Co}^{4+}$ ratio being 0.75. For this concentration, charge ordering can be obtained if the Co^{4+} ions occupy the centre position in a Kagome lattice and the Co^{3+} ions occupy the corner positions as shown in figure 7b. With the charge ordering of Co ions in the Kagome lattice, the Na ions in the adjacent layer, to avoid the proximity of Co^{4+} ions, could jump to Na(1) positions directly above Co^{3+} . This situation is shown schematically in figure 7c. This could account for the changes in relative intensities (see figure 5) as also the abrupt drop in the mode frequency of the out-of-plane Na modes, as seen in figure 4. This argument is in line with the earlier report [3] that the occurrence of the charge ordered insulating state seems to require a strong interaction between the Na ions and the holes in the CoO_2 layers. It is interesting to note that while the out-of-plane Na modes show dramatic changes coincident with the MIT, no significant effects are observed in the cobalt modes.

To summarize, the present IR experiments show changes in Na mode frequencies and intensities, that has been rationalized as arising due to charge ordering in the CoO₂ layer. This charge ordering is induced by Ni doping, in the region of the phase diagram ($x \sim 0.75$), where magnetic instability is expected. It would be worthwhile to follow up on the above infrared studies, using experimental techniques such as neutron diffraction to look for structural changes, viz., changes in bond lengths and site occupancies across the MIT in Ni-doped Na_{0.7}CoO₂.

Acknowledgments

This paper, in part, is based on the invited talk delivered by one of the authors (CSS) at the Golden Jubilee session of the DAE Solid State Physics Symposium at BARC, Mumbai. CSS would like to thank the organizers of DAE-SSPS for this unique opportunity.

References

- [1] I Terasaki, Y Sasago and K Uchinokura, *Phys. Rev.* **B56**, R12685 (1997)
- [2] K Takada, H Sakurai, E Takayama-Muromachi, F Izumi, R A Dilanian and T Sasaki, *Nature (London)* **422**, 53 (2003)
- [3] M L Foo, Y Wang, S Watauchi, H W Zandbergen, Tao He, R J Cava and N P Ong, *Phys. Rev. Lett.* **92**, 247001 (2004)
- [4] N Gayathri, M Premila, A Bharathi, V S Sastry, C S Sundar and Y Hariharan, cond-mat/0507045
- [5] W Y Zhang, H C Yu, Y G Zhao, X P Zhang, Y G Shi and Z H Cheng, *J. Phys. Condens. Matter* **6**, 4935 (2004)
- [6] M Yokoi, H Watanabe, Y Mori, T Moyoshi, Y Kobatashi and M Saito, *J. Phys. Soc. Jpn.* **73**, 1297 (2004)
- [7] N L Wang, Dong Wu, G Li, X H Chen, C H Wang and X G Luo, *Phys. Rev. Lett.* **93**, 147403 (2004)
- [8] G Baskaran, cond-mat/0306569, cond-mat/031; *Phys. Rev. Lett.* **91**, 097003 (2003)
- [9] Q Huang, M L Foo, R A Pascal Jr, J W Lynn, B H Toby, Tao He, H W Zandbergen and R J Cava, *Phys. Rev.* **B70**, 184110 (2004)
- [10] Q Huang, M L Foo, J W Lynn, H W Zandbergen, G Lawes, Yayu Wang, B H Toby, A P Ramirez, N P Ong and R J Cava, *J. Phys. Condens. Matter* **16**, 5803 (2004)
- [11] H W Zandbergen, M Foo, Q Xu, V Kumar and R J Cava, *Phys. Rev.* **B70**, 024101 (2004)
- [12] J L Gavilano, D Rau, B Pedrini, J Hinderer, H R Ott, S Kazakov and J K Karpinski, *Phys. Rev.* **B69**, 100404 (2004)
- [13] A Chainani, T Yokoya, Y Takata, K Tamasaku, M Taguchi, T Shimojima, N Kamakura, K Horiba, S Tsuda, S Shin, D Miwa, Y Nishino, T Ishikawa, M Yabashi, K Kobayashi, H Namatame, M Taniguchi, K Takada, T Sasaki, H Sakurai and E Takayama-Muromachi, cond-mat/0312293
- [14] Y G Shi, Y L Liu, H X Yang, C J Nie, R Jin and J Q Li, *Phys. Rev.* **B70**, 052502 (2004)
- [15] H X Yang, C J Nie, Y G Shi, H C Yu, S Ding, Y L Liu, D Wu, N L Wang and J Q Li, cond-mat/0412578

- [16] G Caimi, L Degiorgi, H Berger, N Barisic, L Forro and F Bussy, cond-mat/0404400
- [17] N L Wang, P Zheng, D Wu, Y C Ma, T Xiang, R Y Jin and D Mandrus, *Phys. Rev. Lett.* **93**, 237007 (2004)
- [18] C Bernhard, A V Boris, N N Kovaleva, G Khaliullin, A V Pimenov, Li Yu, D P Chen, C T Lin and B Keimer, *Phys. Rev. Lett.* **93**, 167003 (2004)
- [19] S Lupi, M Ortolani and P Calvani, *Phys. Rev.* **B69**, 180506R (2004)
- [20] S Lupi, M Ortolani, L Baldassarre, P Calvani, D Prabhakaran and A T Boothroyd, *Phys. Rev.* **B72**, 024550 (2005)
- [21] Zhenyu Li, Jinlong Yang, J G Hou and Qingshi Zhu, *Phys. Rev.* **B70**, 144518 (2004)